Available online at www.pelagiaresearchlibrary.com

Pelagia Research Library

Der Chemica Sinica, 2017, 8(1):83-92

ISSN : 0976-8505
CODEN (USA): CSHIA5

Influence of Relative Humidity on The Morphology of Electrospun Polymer Composites

Yanet E. Aguirre-Chagala[1], Víctor M Altuzar-Aguilar[1,2], Jorge G. Domínguez-Chávez[3], Ernesto F. Rubio-Cruz[4] and Claudia O. Mendoza-Barrera[1,2]*

[1]*Laboratorio de Nanobiotecnología, MICRONA, Universidad Veracruzana, Boca del Río, Veracruz, 94294, Mexico*
[2]*Facultad de Ciencias Físico-Matemáticas, Benemérita Universidad Autónoma de Puebla, Puebla, Puebla, 72570, Mexico*
[3]*Facultad de Bioanálisis, Universidad Veracruzana, Veracruz, Veracruz, 91700, Mexico*
[4]*Facultad de Ingeniería, Universidad Veracruzana, Boca del Río, Veracruz, 94294, Mexico*

ABSTRACT

Polymeric composites have a potential application in tissue engineering. Several parameters of the electrospinning technique and their impacts have been studied. But, the humidity effects during the process are far less explored. Two ranges of controlled humidity 30-35 and 70-75% were established to relate the impact on the fiber morphology. Binary and complex composites were fabricated by blending biopolymers and a ceramic constituent. We chose poly(ethylene oxide)/mesquite gum, poly(vinylpyrrolidone)/mesquite gum/hydroxyapatite, and poly(ethylene oxide)/chitosan/ hydroxyapatite systems, as a comparative study. In particular, mesquite gum is a biocompatible material that has not been investigated as a biocomposite and offers potential physicochemical properties. On the other hand, chitosan offers good properties for tissue engineering and has been extensively studied, however its processing remains a challenge and covers a great interest. The diameter sizes and morphology were assessed by using scanning electron microscopy (SEM) and the chemical structure was analyzed by Fourier transform infrared spectroscopy (FT-IR). Nano-scaffolds obtained, yielded nanofibers, nets and spindle-like fibers, their resultant dimensions were from 89 nm to 388 nm. These results obtained describe how much different morphological features can be induced under low and high humidity during fiber fabrication which is crucial for its later application in biological studies.

Keywords: Electrospinning; Humidity; Morphology; Hydroxyapatite; Mesquite gum

INTRODUCTION

Electrospinning is a very highly widespread technique to process polymer solutions into continuous fibers with diameters ranging from <3 nm to over 1 μm. The effectiveness of this technique facilitates the fabrication of scaffolds for biomedical applications among other fields of interest. [1]. Briefly, electrostatic fiber formation is a method where a high external electrical field is applied to a polymer solution in a capillary, possessing sufficient chain overlap and molecular entanglement to constrain the chain motion, where its velocity is adjusted by a pump. When the surface tension is overcome by the electrical force, the hemispherical surface deformation of the polymeric fluid creates the Taylor cone, allowing the jet to travel towards the grounded target substrate, meanwhile the solvent evaporates and the dry fiber is collected into an oppositely charged plate [2, 3].

Many factors can influence the overall process outcome and fiber morphology; these parameters can be divided into: electrospinning parameters (distance to collector, voltage, feed rate, etc.) [4], solution properties (polymer molecular weight, viscosity, conductivity, etc.) [5] and ambient conditions (humidity, temperature, etc.) [6]. Among environmental conditions, relative humidity percent (RH%) can affect the fiber structure and diameter size distributions, making the process more difficult at high water concentrations [7]. While there are experimental studies of electrospun fibers covering a variety of electrospinning parameters and solution properties, relative humidity has not been sufficiently investigated.

Microstructure of electrospun fiber under air may be influenced by solvent properties and hydrophobicity/hydrophilicity polymer; these issues interplay a role with humidity and the outcomes are not always predictable [8]. Relative humidity implies that in the atmosphere exist water molecules in vapor phase which promote the raise of partial pressure of water vapor. This phenomenon has an impact on the evaporation rate of the solvent from polymer solutions. At higher relative humidity the evaporation rate of the solvent decreases and consequently perturbs the ideal jet diameter during the trip to the collector. On based water solutions, have been observed thinner fibers at higher relative humidity and thicker fibers with the decrease of relative humidity [9, 10]. The solvent evaporation depends on the moisture content and the local viscosity in the polymer jet changes, so the fiber diameter varies as well [11]. In other words, the solidification of the polymer is faster at low humidity after applying a certain voltage, and consequently the stretching of polymer chains in short time is induced. As a result, the diameter size is smaller and more homogeneous at low humidity than at high humidity, in some particular systems. A mixture of nitrogen and air, allow controlling the moisture in the atmosphere of the electrospinning process and therefore to tune the morphology. Earlier studies have observed specific morphologies in an ample range of moisture in the air, such as beaded fibers, spindle-like fibers, porous surfaces, at micro- and nanoscale [12].

The aim of this work is to know how the relative humidity impacts the morphology of electrospun fibers as well as to investigate the role of humidity as a function of the diameter sizes. Here, we describe the morphology of the electrospun fibers of distinct polymer blends, including mesquite gum and chitosan biopolymers, polyethylene oxide and polivinylpyrrolidone, and/or hydroxyapatite. Mesquite gum (*Prosopis spp*.) is not yet commercially available; nevertheless these leguminous seeds offer a source of polysaccharide. This biopolymer is a neutral polymer; their main component is the galactomannans family. The chemical structure of this polysaccharide has a main mannose chain linked by $\beta(1\rightarrow4)$ glycosidic bonds with galactose branches joined by $\alpha(1\rightarrow6)$ bonds. Because of their functional properties and for their minimally toxicity, potential applications have been reported in textile, alimentary and pharmaceutical industries [13]. The average molecular weight of galactomannans from mesquite gum seeds has been estimated between 9×10^5 g/mol and 1.2×10^6 g/mol, which indicates that they can be used as a thickening agent [14, 15]. On the other hand, chitosan is a copolymer of (1→4)-2-amino-2-deoxy-β-D-glucan and (1→4)-2-acetamido-2-deoxy-β-D-glucan and is the second most abundant biopolymer in nature. Its structure is capable of forming inter- and intramolecular hydrogen bonds. Chitosan molecules behave like a cationic polyelectrolyte, thanks to the protonation of the amine groups attached to their backbone. In addition, CH exhibits antimicrobial activity and wound healing properties [16]. Because of its poor mechanical properties, electrospinning of chitosan presents many challenges. In an attempt to overcome this issue, several authors selected biopolymers o synthetic polymers as co-spinning agents [11, 17, 18], for instance PEO can facilitate polymer entanglement due to its linear structure with flexible and long chains. A major inorganic component in natural bone is the hydroxyapatite, furthermore is the most stable calcium phosphate under physiological conditions; furthermore this ceramic enhance the mechanical properties of the resultant composites [19].

The importance of using hybrid polymeric systems relies on the fact that their properties might be readily modulated by a versatile and low-cost technology, giving a range of materials with distinct physicochemical properties. Understanding the effect of humidity, enables the controlled formation of biocomposite systems, providing a systematic method for tissue engineering applications [19-22].

MATERIALS AND METHODS

Materials

Poly (ethylene oxide) (PEO, M_w=600,000 g/mol), polivinylpyrrolidone (PVP, M_w=360,000 g/mol), chitosan medium molecular weight (CH, M_w=190,000-310,000 g/mol, deacetylation degree: 75-85%), Triton X-100, hydroxyapatite nanopowder (HP, particle size <200 nm BET) were obtained from Sigma-Aldrich. Mesquite gum seeds (MG) were purchased from a local supplier in the State of Tamaulipas, Mexico and were manually gathered, separated and stored. Ethyl alcohol and acetic acid were purchased from J.T. Baker and used as received. Deionized water was purified in a Barnstead Nanopure system to a final electrical resistivity of 18.2 MΩ-cm.

Preparation of fibers

During the fabrication of all fiber systems, relative humidity and temperature were monitored with Labview® Software to achieve two different conditions of relative humidity percent (30-35 and 70-75 RH%). In the case of using low humidity, the glovebox was degassed with nitrogen, where further the samples were collected [9]. The polymer aqueous solution of interest was transferred into a 5 mL plastic syringe with a caliber stainless steel needle of 21G × 32

mm and right after was placed in a programmable injection pump (KD scientific™, model: 780100V), located outside the glovebox. The needle tip was connected to the anode of the voltage power supply (Gamma High Voltage Research, model: ES60p-20W/DAM), the cathode was attached to a 12 cm × 12 cm aluminum sheet as a collector, and the needle distance to the collector was fixed to 12 cm [23]. Finally, the fibers were stored in a desiccator for further analysis.

Poly(ethylene oxide)/mesquite gum (PEO/MG) system

PEO/MG polymer blends were prepared at weight ratios of 80/20, 70/30, 50/50, and 20/80, with a total polymer weight of 1 g (10% w/v). To prepare a solution of 70/30, PEO (0.7 g) was dissolved in 10 mL deionized water under vigorous stirring, and then mesquite gum (0.3 g) was slowly added [24]. All solutions and the electrospinning process were carried out at room temperature. The feed rate was 0.3 mL/h, the applied voltage was 20 kV, and the humidity values were of 30-35 and 70-75%. Fibers were labeled with PEGX/MGY-(A or N) name; where X corresponds to the weight ratio of PEG; Y is the subtraction of 1-X, which indicates the weight ratio of MG; A specifies in air condition (70-75 RH%) and N specifies in nitrogen (30-35 RH%).

Poly(vinylpyrrolidone)/mesquite gum/hydroxyapatite (PVP/MG/HP) system

Briefly, hydroxyapatite (0.01 g to obtain 2 wt%) was dissolved in 10 mL of 50% (v/v) ethanol solution for over 24 h at room temperature at different weight fractions (0.5, 1, 2, and 3 wt%). Then, PVP (0.5 g) was added under magnetic stirring for about 1 h. Later, mesquite gum (0.5 g) was added and allowed to dissolve, a total polymer weight was kept constant to 1 g (10% w/v) as well as the weight polymer ratio of PVP/MG=50/50. The mixture was loaded into the syringe and fed to 0.4 mL/h, using a voltage of 20 kV, and 30-35 and 70-75 RH% [24]. Fibers were labeled with PXMY/(A or N) name; where X corresponds to the weight ratio of PVP; Y is the subtraction of 1-X, which indicates the weight ratio of MG; A specifies in air condition (70-75 RH%) and N specifies in nitrogen (30-35 RH%).

Poly(ethylene oxide)/chitosan/hydroxyapatite (PEO/CH/HP) system

A determined weight polymer ratio was fixed at PEO/CH=80/20, where the total polymer weight was of 0.3 g (3% w/v). Different hydroxyapatite weight contents were used to prepare all solutions (0.5, 1, 2 and 3 wt%) and triton X-100 (0.9, 0.5 and 0.2 mM) [25]. To prepare a solution, chitosan (0.06 g) was slowly added into 10 mL of 10% (v/v) acetic acid solution and then PEO (0.24 g) was incorporated under vigorous stirring and allowed to dissolve at room temperature [17]. Afterwards, hydroxyapatite (6 mg to obtain 2 wt%) was loaded in the polymer solution followed by triton X-100 (10.5 µL for 0.9 mM) addition. Final solution was sealed and allowed to dissolve for above 24 h. The electrospinning process was performed with a flow rate of 0.5 mL/h and 23 kV as voltage, at 30-35 and 70-75 RH%. Fibers were labeled with PC/XHYT(A or N) name; where X corresponds to the weight ratio of hydroxyapatite; which indicates the concentration mM of triton X-100; A specifies in air condition (70-75 RH%) and N specifies in nitrogen (30-35 RH%).

Characterization

Images of the electrospun composites were obtained with a JEOL model JSM-7600F scanning electron microscope. The samples were prepared by placing a conductive carbon double-sided tape. In the case of PEO/MG samples, the voltage used was 1 kV; for PVP/MG/HP samples were 2 kV, whereas to observe PEO/CH/HP fibers 0.5 kV were used. A x10,000 and x5,000 magnification was used to analyze all images. The fiber diameter distributions were determined using ImageJ® Software, by measuring 100 fibers for each one. Elemental analysis was performed by energy dispersive spectroscopy (EDS), with an acceleration voltage of 6 kV. FT-IR spectra were recorded on a Thermo Scientific spectrometer (model Nicolet Isso FT-IR) with ATR apparatus, in the 4000-500 cm^{-1} range, with a resolution of 4 cm^{-1} and 32 scan per minute. Thermal properties were recorded by differential scanning calorimetry (DSC) Q2000 TA Instruments, with a heating rate of 10°C/min from 50 to 200°C.

Statistical analysis

Data were analyzed by one-way analysis of variance (ANOVA) in conjunction with Tukey's post hoc test for multiple comparisons. Differences were considered with significant at $p<0.05$.

RESULTS AND DISCUSSION

Poly(ethylene oxide)/mesquite gum (PEO/MG) system

Morphology of fibers

A lower content of mesquite gum promotes the fiber formation, while specifically at 80% of content we observed the

fusion of fibers, possibly as a result of far more interactions of hydrogen bonds (**Figure 1**). From our data, it was found that independently of the relative humidity, at the highest content (80% w/wp) of PEO to the lowest (50% w/wp), the diameter decreases; at 30-35 RH% from 256 ± 139 nm to 197 ± 78 nm, and at 70-75 RH% from 388 ± 111 nm to 268 ± 70 nm; whereas their standard deviations exhibited the same effect with broader values.

The moisture of the environment affected directly on the fiber diameters (**Figure 2A**, $p<0.05$). Despite the high humidity (70-75 RH%), the distributions of the average diameters were wider but the morphology was still similar at the low humidity range (30-35 RH%). In either of the ranges, the surfaces were smooth and the bead formation was completely absent. In addition, this polymer blend system would allow performing a feasible process because of the environmentally friendly, easy manipulation and low cost as well. In this context, this biocomposite is an attractive candidate for future tissue engineering applications, particularly PEG8/MG2-N sample which formed net morphology instead of long fibers (**Figure 1E**).

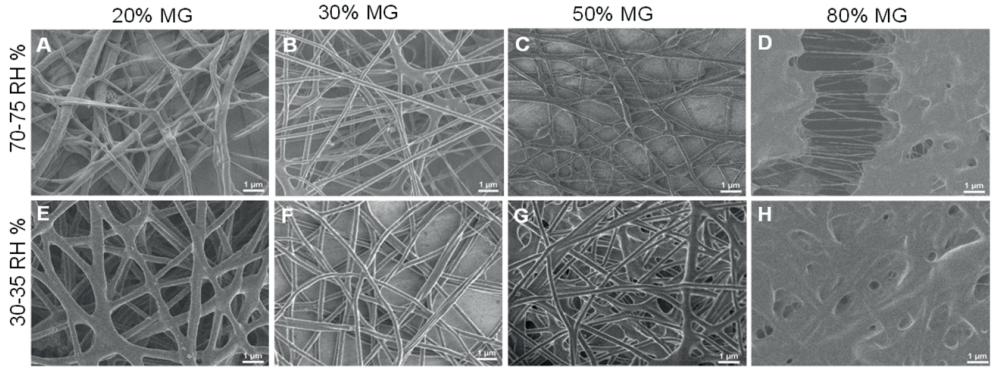

Figure 1: SEM micrographs of PEO/MG fibers at 70-75 and 30-35 RH%, x10,000, 1.0 kV.

As it was previously mentioned, the diameter size had a small significance (**Figure 2A**, $p<0.05$) with the weight fraction content of mesquite gum and PEO incorporated [17]. Raising the humidity helped decrease the diameter, which is in agreement with other authors [11]. At higher concentration of water molecules in the atmosphere during the electrospinning process, the water evaporation in the polymeric jet is slower and therefore solidifies more slowly. Aside from these considerations, the hydrophilicity factor contributes to the absorption of water molecules, which may increase the wettability of the polymer jet and as consequence to obtain small fibers. For instance, when a PEO solution is used, the fabrication of the well-made fibers is not completely achieved above 50 RH%, relating such phenomenon to its hydrophilic chains of the linear polymer [9]. Indeed, the non-ionic character of both polymers hinders a marked impact on the fiber microarchitecture, originated by their neutral chemistry and branched nature of the galactommans, promoting a good spinnability of the polymeric solution.

Chemical structure of fibers

The FT-IR spectra of pure polymers and PEO5/MG5 fiber are shown in **Figure 2B**. The characteristic bands are assigned as follows, a broad band centered about 3350 cm^{-1} is attributed to the H-bonded stretch of -OH groups from MG, the band at 2883 cm^{-1} to the antisymmetric stretching of $-CH_3$, $-CH_2-$ vibration, the band 1456 cm^{-1} is assigned to the scissors vibration mode of the methylene $-CH_2-$ originated from the polymer backbone of PEO, the sharp band at 1340 cm^{-1} corresponds to the methyl $-CH_3$ group deformation mode from PEO. The absorption bands at 1279 cm^{-1} and 1241 cm^{-1} are originated from C-O-C antisymmetric stretch. A strong band at 1094 cm^{-1} corresponds to the stretch C-O mode, indicating the presence of polyether. Other characteristic absorption bands are observed in the 1183-926 cm^{-1} region, associated with several vibration modes of C-O and C-O-H groups of carbohydrates [15].

Figure 2C displays the FT-IR spectra at 0, 20, 30, 50, 80 and 100% composition of mesquite gum. Depending upon which types of functional groups are present in the polymer chains, it is possible to have different intra and intermolecular interactions, such as hydrogen bonding. We observed a shift of the main centered band assigned to the mesquite gum at 989 cm^{-1}, attributed to the C-O-H vibrations in cyclic compounds [26]; and its intensity decreases as a result of lower content of the polysaccharide.

As shown in **Figure 2D**, all fibers presented hydrogen bonding interaction within the matrix. The ratio of the absorption intensities at 3350 and 989 cm-1 associated with mesquite gum, were used to elucidate the level of molecular interaction H-bonds. The reason of these changes for this ratio might be explained by the decreasing of hydrogen bonds between polysaccharide chains upon the presence of PEO molecules, leading to a local variation in

the macromolecules packing; which would modify the formation of H-bonds and as a consequence the intensity of the broad band 3350 cm-1 would decrease.

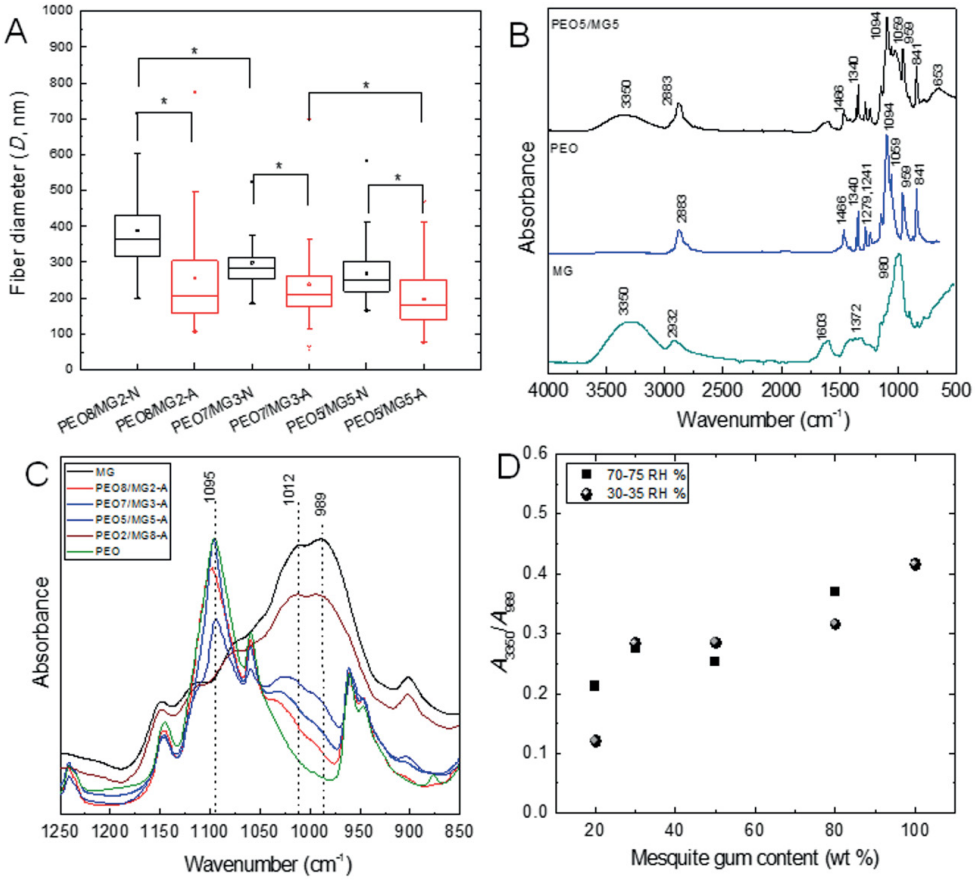

Figure 2: (A) Diameters (*p<0.05) (B-C) FT-IR spectra (D) Absorbance intensity ratio of H-bonds in PEO/MG fibers.

Poly(vinylpyrrolidone)/mesquite gum/hydroxyapatite (PVP/MG/HP) system

In this system, we previously assessed the solvent in order to know the spinnability of ceramic and polymer solution in water, 50% (v/v) ethanol and acetic acid 5% (v/v). **Table S1** shows the conditions used for the electrospinning process and the values of the atomic relations of P/N by EDS. Our findings suggested that the more appropriate solvent for electrospinning was 50% (v/v) ethanol for 1 wt% HP in the solution, the atomic relation of P/N obtained was 0.00925, closer to the theoretical value of 0.0131.

Morphology of fibers

SEM micrographs are presented in **Figure S1**, where it can be observed that bead morphology is less present using ethanol as co-solvent (**Figure S1B**), improving the spinnability of the complex solution. In the case of the variation of the polymer weight fraction ratio (w/w %) as PVP/MG=80/20, 50/50 and 20/80, having a constant hydroxyapatite concentration, there was a similar morphology at 50/50 and 20/80. At higher concentration of PVP (80/20), the fiber diameter was increased by a factor of 2 (from 52 ± 12 to 101 ± 62 nm). Composites in all cases exhibited mostly smooth fibers and some beads, of which beaded forms decreased when PVP concentration increased (**Table S2** and **Figure S2**). In all cases, fibrous morphology was observed in nanoscale; however, the presence of large and tiny beads was noticeable (**Figure 3**). We observed similar morphology at 70-75 RH%, rendering diameter values slightly greater than the corresponding ones at 30-35 RH% (**Figure 4A**, p<0.05). It is thought and supported that the lack of viscosity of the polymer solution (PEO M_{wPEO}=600 kDa versus PVP M_{wPVP}=360 kDa, were employed for 10% w/v solutions) could be the reason of the bead formation about 300-500 nm of diameter. Comparing results of both systems, PEO/MG and PVP/MG/HAP, we consider that the hydrophilic nature and neutral character of these polymers (MG, PVP, and PEO) play an important role, where formation of well-defined fiber can take place even under high humidity environmental conditions.

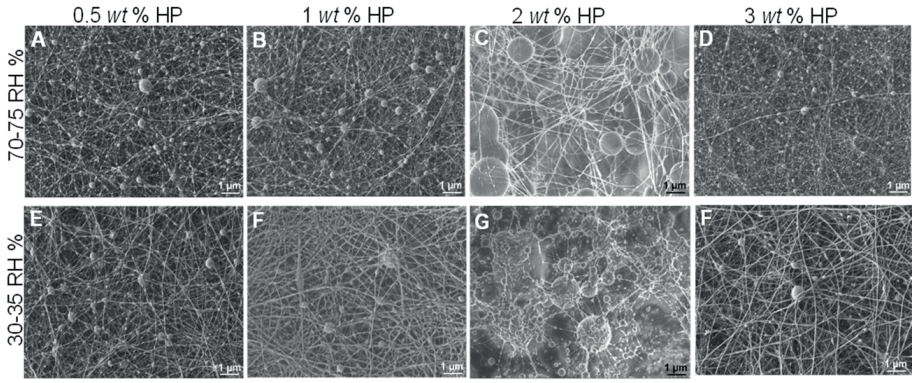

Figure 3: SEM images of electrospun PVP/MG/HP fibers at 70-75% relative humidity, x10,000, 2.0 kV.

Chemical structure of fibers

Spectra of individual component and P5M5/1HA fiber are displayed in **Figure 4B**. The absorption bands from mesquite gum were previously described. As it is well-known, hydroxyapatite PO_4^{3-} ions have four vibration bands; two strong bands are observed at 1021 and 568 cm^{-1}, the less intense bands at 1087, 960, 601 and 630 cm^{-1} are attributed to stretch vibration mode [27]. The spectrum of P5M5/1HA fiber showed a broad band at 3350 cm^{-1} corresponding to the -OH groups, whereas the band 2921 cm^{-1} was assigned to the antisymmetric -CH_2- stretching vibration band of the polymer backbone. A sharp absorption band positioned at 1647 cm^{-1} was associated with the stretching C=O vibrations (amide I band) presented in tertiary amide of PVP lactam. The contribution of stretching C-N vibration was observed at 1422 and 1288 cm^{-1}, characteristic of lactam ring. Another broad and strong band at 1017 cm^{-1} was assigned to the bending C-H vibration modes as well as the centered band around 837 cm^{-1} originated from C-N vibrations [28].

The interaction of the polymer chains was analyzed in the FT-IR region (**Figure 4C**) selected from 1350 to 900 cm^{-1}. Intensity of the absorption band at 989 cm^{-1} (from MG) increased as much as the weight percent content of mesquite gum was incorporated, detecting a shift of this band to higher wavenumber about ~12 cm^{-1}, coupled with the reduction of the band at 1270 cm^{-1} (from PVP). This might be attributed to molecular interaction of each given component between the lactam ring and C-O-H groups, possibly because of the attraction of C-O-H proton of secondary and primary alcohols, promoting the lower electron density of C=O bond of the lactam [29]. However, carbonyl absorption band at 1647 cm^{-1} of PVP did not shift to new frequency absorption and only the stretch C-N vibration was detected.

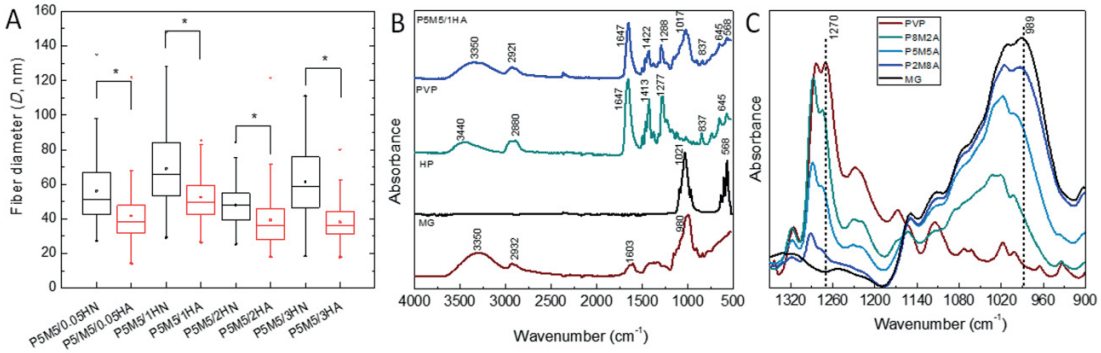

Figure 4: (A) Fiber diameters of P5M5/H system a two RH% (*p<0.05). (B-C) FT-IR spectra of fibers.

Poly(ethylene oxide)/chitosan/hydroxyapatite (PEO/CH/HP) system

Morphology of fibers

For this system, the addition of a nonionic surfactant as Triton X-100 was used to improve the spinnability of the solution due to its capability to lower surface and interfacial tension [30]. The resulting morphologies obtained in air (70-75 HR%) are shown in **Figure 5** and **Figure S4A**. All composites displayed a dendritic morphology at all hydroxyapatite weight fractions including those at distinct molarity of triton [31]. In general, high humidity (because water vapor is electrically conductive) affects the charge distribution on Taylor cone, producing a decrement of the surface charge density, which can entail defects on fiber formation. The interaction of the surrounding high content of water vapor in the atmosphere modified the microarchitecture of the fibers. Also, a lowering on the fiber diameters was exhibited; similar to the systems previously discussed (PEO/MG and PVP/MG/HP).

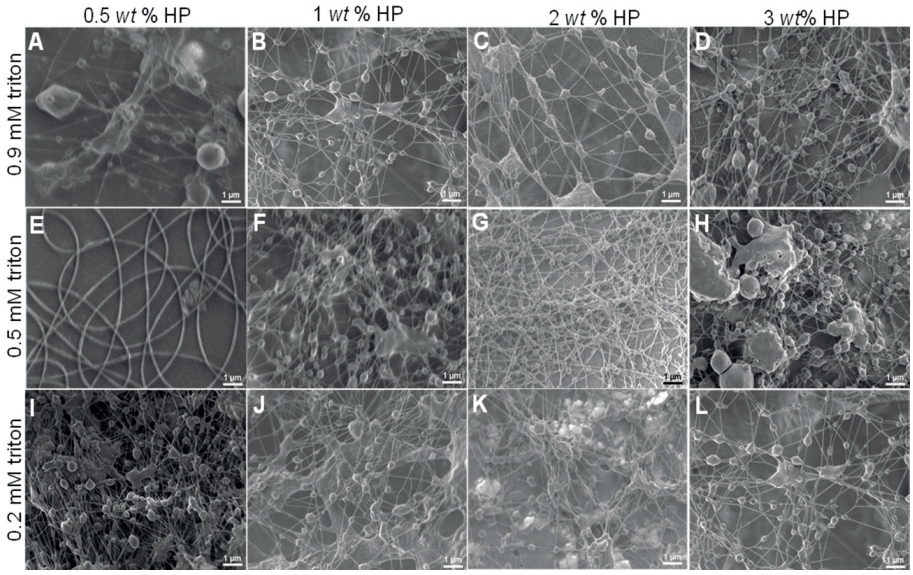

Figure 5: SEM images of PEO/CH/HP fibers. All samples were prepared at 70-75 RH%, x10,000, 0.5 kV.

For the sake of comparison, those composites made of non-ionic polymers (GM, PVP and PEO) did not demonstrate a morphology conversion to lower and higher humidity, in contrast to the ionic polymer (CH) [4]. It suggests that the solution conductivity might significantly impact the morphology in relation to the variations of humidity; thereby cationic nature of chitosan would promote more dendritic morphology.

In nitrogen (30-35 RH%), uniform and smoother fibers were yielded, which allowed us to control better the morphology. Spindle-like fibers were formed by using 2 and 3 wt% HP at 0.9 mM triton (**Figure 6C** and **Figure 6D**, respectively), but to lower triton concentration, these features were not observed [32]. The reason is possibly because the self-assembly of 0.9 mM triton X-100 solutions is more thermodynamically stable at 0.2 mM, and the micellar solution could serve as hydroxyapatite carrier. It is likely that triton above its critical micellar concentration (C_{cmc}~0.22-0.9 mM) can provide sites for specific embedded clusters of hydroxyapatite. Thus, it is of high importance, the surfactant concentration in order to pursue higher control of morphology for these composites. Less than 1 wt% hydroxyapatite (**Figure 6A, 6B, 6E, and 6F**), the fiber structure had a significant change in low humidity, for both triton concentrations (0.2 and 0.9 mM). Below the critical micellar concentration the interactions between the two different chemical species (surfactant-polymer) depend on hydrophobic interactions and/or H-bonds [33].

Diameter values were different on the RH% range during the electrospinning process. Upon high RH% the diameter values were lower than the values obtained upon low RH% (**Figure 7**). This observation was similar for each case of triton concentration. Besides, it can be clearly observed that the influence of triton content and hydroxyapatite incorporated did not show a significance difference in their diameter values. The decrease of the diameter matched with the previously systems discussed, thus confirming the same observations.

Chemical structure of fibers

FT-IR spectra are presented in **Figure 8A**, which shows all typical bands expected within the composite. A wide band centered at 3360 cm^{-1} corresponds to hydroxyl groups, stretching of methyl and methylene groups (-CH_3, -CH_2-) were confirmed at 2879 cm^{-1}, as well as the typical bands at 1646 cm^{-1} for the C=O stretch mode vibration and 1574 cm^{-1} for -NH deformation mode for secondary amide. Also, to corroborate the presence of amide and amine groups, the C-C-N bending mode vibration at 1279 cm^{-1} was detected. The main band at 1098 cm^{-1} is a convolution of the three components of the composite, including C-O-C stretching vibration, C-O- stretching vibration of secondary and primary alcohols, and stretching vibration of P=O (belonging to the phosphate group). We did not discard H-bonds between P=O, -NH_2 and –OH groups, based on its attainability to provide interaction sites with other functional groups. However, as it was showed on the spectra, all absorbance bands are mainly dominated by PEO rather than the others ones, while induced for the low content of hydroxyapatite to prepare the composites.

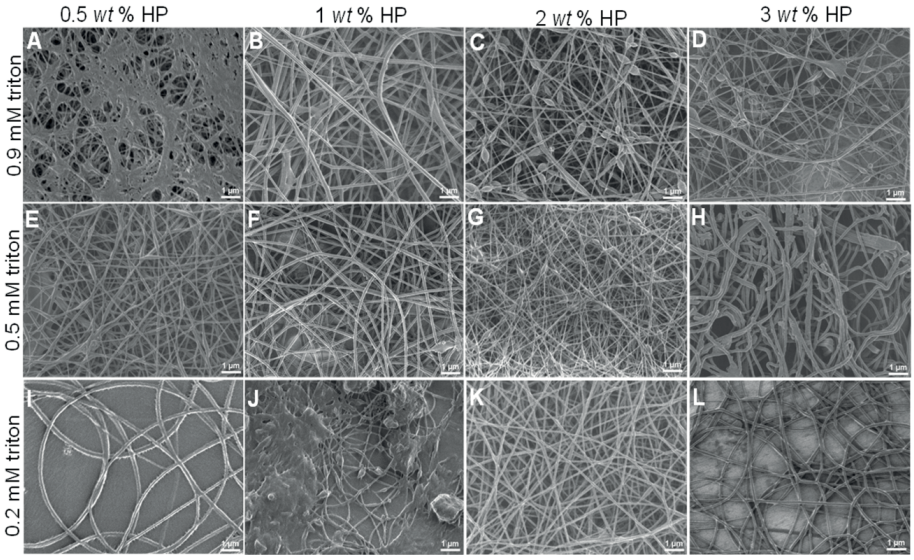

Figure 6: SEM images of PEO/CH/HP fibers. All samples were prepared at 30-35 RH%, x10,000, 0.5 kV.

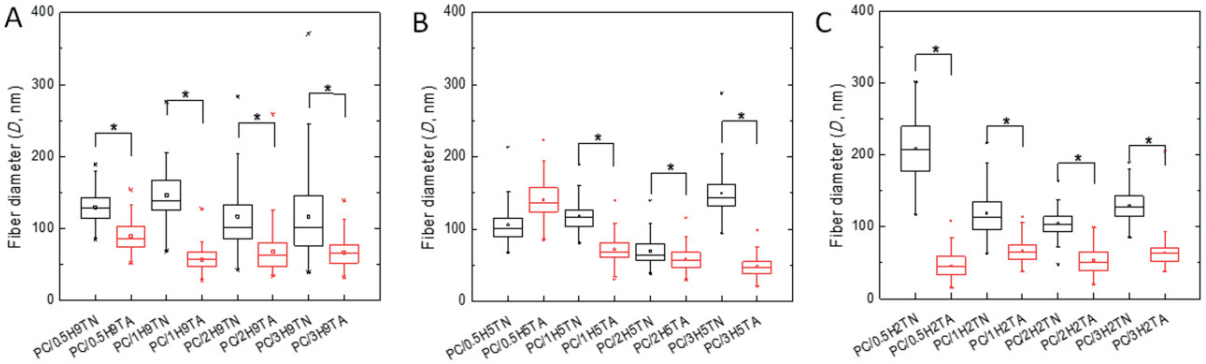

Figure 7: Diameters versus HP content at different RH%: (A) 9mM, (B) 5mM and 2mM triton, (*p<0.05).

Thermal study

The thermal properties of all samples of the system were examined by DSC. The thermograms are presented in **Figure 8B**. We observed a peak transition at 66.5°C, which indicates the melting temperature (T_m) of PEO. All T_m showed a shift at about ~ Δ5°C to lower temperature, associated with the chitosan incorporated. Chitosan melting temperature has been reported at 82.2°C, whilst in this work the chitosan content was less than PEO (20 vs 80 wt%, respectively), its individual endothermal peak was not clearly evidenced, as a result only a broad peak was observed [30]. The melting enthalpy (ΔH_m) is an indicative of semicrystallinity, where the ΔH_m for PEO powder is 52.5 J/g (**Table 1**). Fibers presented slightly higher ΔH_m values, indicating that the molecular arrangement resulted more ordered with the incorporation of hydroxyapatite. In general, polymer solutions at high concentrations have macromolecular entanglement chains, in which their crystal domains prevail. When a polymer solution is subject to electrostatic force, a stretching of the polymer chains is experimented. Accordingly, if polymers are used to fabricate fibrous structures by electrospinning, we can ascribe a reduction of crystallinity. Notwithstanding, our DSC results indicated more crystallinity in the PEO/CH/HP composites [34]. The fibers spun in nitrogen and in air had a similar thermal behavior, and the onset temperature of degradation (T_d) exhibited values between 174-189°C, suggesting that low content of ceramic constituent enhanced the thermal stability of the composite, in comparison to PEO stability at 171°C [35]. On the other hand, we expected that T_d will heighten from 0.5 to 3 wt% of HP, but this assumption was not validated in samples prepared in nitrogen or under air, remaining practically the same degradation temperature.

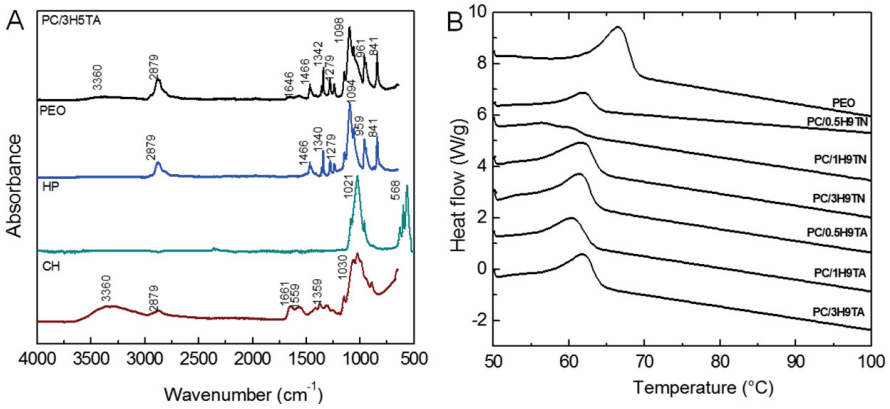

Figure 8: (A) FT-IR spectra. (B) Thermograms of fibers, measured by DSC.

Table 1: Thermal analysis measured by DSC.

Sample	T_m (°C)	ΔH_m (J/g)	T_d (°C)
PC/0.5H9TA	61.4	57.6	175.5
PC/1H9TA	60.5	52.3	180.0
PC/3H9TA	62.1	55.6	178.1
PC/0.5H9TN	62.1	60.0	174.6
PC/1H9TN	56.7	45.3	180.2
PC/3H9TN	61.9	56.9	181.3
PC/0.5H2TA	59.9	41.1	189.8
PC/1H2TA	60.3	54.7	161.3
PC/3H2TA	60.9	55.6	180.2

CONCLUSION

This study reveals that composite morphology and diameter size distributions were susceptible to the moisture content in the atmosphere. More uniform and thicker fibers were generated under nitrogen/air mixture (30-35 relative humidity percent). The difference of the humidity impact was found to be highly dependent on polymer nature. Knowing the role of the RH% range in a specific polymer system, it is possible to take the impact of its influence into account and conduct to a straightforward approach of the process. As it is shown in our results, from cationic polymer solutions, dendritic to fibrous composites were obtained as a result of the unbalance of electrostatic forces during the electrospinning process; however, when neutral polymer solutions were used the impact on composite morphology happened to be less relevant.

ACKNOWLEDGEMENT

We thank Universidad Veracruzana for the facilities and Josué F. Perzábal Dominguez, Ángel E. Peto Olvera, Miguel J. Herrera-Montalvo and Angélica Gutierrez-Franco for their technical support. YEAC thanks CONACYT-Mexico (CVU No. 232954) for the financial support (Project No. 29144). This project was partially supported by SEP-PROMEP Project Redes 2015 (UV-CA 314, BUAP-CA 34 and CICATA-IPN).

REFERENCES

[1] Reddy VJ, Radhakrishnan S, Ravichandran R, Mukherjee S, Balamurugan R, et al. (**2013**) Nanofibrous structured biomimetic strategies for skin tissue regeneration. *Wound Repair Regen* 21: 1-16.

[2] McKee MG, Wilkes GL, Colby RH, Long TE (**2004**) Correlations of solution rheology with electrospun fiber formation of linear and branched polyesters. *Macromolecules* 37: 1760-1767.

[3] Shenoy SL, Bates WD, Frisch HL, Wnek GE (**2005**) Role of chain entanglements on fiber formation during electrospinning of polymer solutions: good solvent, non-specific polymer-polymer interaction limit. *Polymer* 46: 3372-3384.

[4] Moutsatsou P, Coopman K, Smith MB, Georgiadou S (2015) Conductive PANI fibers and determining factors for the electrospinning window. *Polymer* 77: 143-151.

[5] Bosworth LA, Downes S (**2012**) Acetone, a Sustainable Solvent for Electrospinning Poly(epsilon-Caprolactone) Fibres: Effect of Varying Parameters and Solution Concentrations on Fiber Diameter. *J Polym Environ* 20: 879-886.

[6] Nezarati RM, Eifert MB, Cosgriff-Hernandez E (**2013**) Effects of Humidity and Solution Viscosity on Electrospun Fiber Morphology. *Tissue Eng Part C-Me* 19: 810-819.
[7] De Vrieze S, Van Camp T, Nelvig A, Hagstrom B, Westbroek P, et al. (**2009**) The effect of temperature and humidity on electrospinning. *J Mater Sci* 44: 1357-1362.
[8] Putti M, Simonet M, Solberg R, Peters GWM (**2015**) Electrospinning poly (epsilon-caprolactone) under controlled environmental conditions: Influence on fiber morphology and orientation. *Polymer* 63: 189-195.
[9] Pelipenko J, Kristl J, Jankovic B, Baumgartner S, Kocbek P (**2013**) The impact of relative humidity during electrospinning on the morphology and mechanical properties of nanofibers. *Int J Pharmaceut* 456: 125-134.
[10] Huang LW, Bui NN, Manickam SS, McCutcheon JR (**2011**) Controlling Electrospun Nanofiber Morphology and Mechanical Properties Using Humidity. *J Polym Sci Pol Phys* 49: 1734-1744.
[11] Kim T, Yang SJ, Sung SJ, Kim YS, Chang MS, et al. (**2015**) Highly Reproducible Thermocontrolled Electrospun Fiber Based Organic Photovoltaic Devices. *ACS Appl Mater Interfaces* 7: 4481-4487.
[12] Casper CL, Stephens JS, Tassi NG, Chase DB, Rabolt JF (**2004**) Controlling surface morphology of electrospun polystyrene fibers: Effect of humidity and molecular weight in the electrospinning process. *Macromolecules* 37: 573-578.
[13] Chaires-Martinez L, Salazar-Montoya JA, Ramos-Ramirez EG (**2008**) Physicochemical and functional characterization of the galactomannan obtained from mesquite seeds (Prosopis pallida). *Eur Food Res Technol* 227: 1669-1676.
[14] Goycoolea FM, Morris ER, Richardson RK, Bell AE (**1995**) Solution Rheology of Mesquite Gum in Comparison with Gum-Arabic. *Carbohydr Polym* 27: 37-45.
[15] Lopez-Franco YL, Cervantes-Montano CI, Martinez-Robinson KG, Lizardi-Mendoza J, Robles-Ozuna LE (**2013**) Physicochemical characterization and functional properties of galactomannans from mesquite seeds (Prosopis spp). *Food Hydrocoll* 30: 656-660.
[16] Wei HQ, Zhang FH, Zhang DW, Liu YJ, Leng JS (**2015**) Shape-memory behaviors of electrospun chitosan/poly(ethylene oxide) composite nanofibrous membranes. *J Appl Polym Sci* 132: 42532.
[17] Pakravan M, Heuzey MC, Ajji A (**2011**) A fundamental study of chitosan/PEO electrospinning. *Polymer* 52: 4813-4824.
[18] Bianco A, Calderone M, Cacciotti I (**2013**) Electrospun PHBV/PEO co-solution blends: Microstructure, thermal and mechanical properties. *Mater Sci Eng C Mater Biol Appl* 33: 1067-1077.
[19] Frohbergh ME, Katsman A, Botta GR, Lazarovici P, Schauer CL, et al. (**2012**) Electrospun hydroxyapatite-containing chitosan nanofibers crosslinked with genipin for bone tissue engineering. *Biomaterials* 33: 9167-9178.
[20] Cheng F, Gao J, Wang L, Hu XY (**2015**) Composite chitosan/poly(ethylene oxide) electrospun nanofibrous mats as novel wound dressing matrixes for the controlled release of drugs. *J Appl Polym Sci* 132: 42060.
[21] Liu L, Yoshioka M, Nakajima M, Ogasawara A, Liu J, et al. (**2014**) Nanofibrous gelatin substrates for long-term expansion of human pluripotent stem cells. *Biomaterials* 35: 6259-6267.
[22] Li Q, Wang XL, Lou XX, Yuan HH, Tu HB, et al. (**2015**) Genipin-crosslinked electrospun chitosan nanofibers: Determination of crosslinking conditions and evaluation of cytocompatibility. *Carbohyd Polym* 130: 166-174.
[23] Zhang YZ, Venugopal JR, El-Turki A, Ramakrishna S, Su B, et al. (**2008**) Electrospun biomimetic nanocomposite nanofibers of hydroxyapatite/chitosan for bone tissue engineering. *Biomaterials* 29: 4314-4322.
[24] Khan WS, Asmatulu R, Eltabey MM (**2013**) Electrical and Thermal Characterization of Electrospun PVP Nanocomposite Fibers. *J Nanomater* 2013: 9.
[25] Liverani L, Abbruzzese F, Mozetic P, Basoli F, Rainer A, et al. (**2014**) Electrospinning of hydroxyapatite-chitosan nanofibers for tissue engineering applications. *Asia Pac J Chem Eng* 9: 407-414.
[26] Cerqueira MA, Souza BWS, Simoes J, Teixeira JA, Domingues MRM, et al. (**2011**) Structural and thermal characterization of galactomannans from non-conventional sources. *Carbohyd Polym* 83: 179-185.
[27] Zhou SB, Zheng XT, Yu XJ, Wang JX, Weng J, et al. (**2007**) Hydrogen bonding interaction of poly(D,L-lactide)/hydroxyapatite nanocomposites. *Chem Mater* 19: 247-253.
[28] Kim GM, Le KHT, Giannitelli SM, Lee YJ, Rainer A, et al. (**2013**) Electrospinning of PCL/PVP blends for tissue engineering scaffolds. *J Mater Sci-Mater M* 24: 1425-1442.
[29] Oh TJ, Nam JH, Jung YM (**2009**) Molecular miscible blend of poly(2-cyano-1,4-phenyleneterephthalamide) and polyvinylpyrrolidone characterized by two-dimensional correlation FTIR and solid state C-13 NMR spectroscopy. *Vib Spectrosc* 51: 15-21.
[30] Kriegel C, Kit KM, McClements DJ, Weiss J (**2009**) Electrospinning of chitosan-poly(ethylene oxide) blend nanofibers in the presence of micellar surfactant solutions. *Polymer* 50: 189-200.
[31] Maeda N, Miao J, Simmons TJ, Dordick JS, Linhardt RJ (**2014**) Composite polysaccharide fibers prepared by electrospinning and coating. *Carbohyd Polym* 102: 950-955.
[32] Maheshwari SU, Samuel VK, Nagiah N (**2014**) Fabrication and evaluation of (PVA/HAp/PCL) bilayer composites as potential scaffolds for bone tissue regeneration application. *Ceram Int* 40: 8469-8477.
[33] Kriegel C, Kit KM, McClements DJ, Weiss J (**2009**) Influence of Surfactant Type and Concentration on Electrospinning of Chitosan-Poly(Ethylene Oxide) Blend Nanofibers. *Food Biophys* 4: 213-228.
[34] Jankovic B, Pelipenko J, Skarabot M, Musevic I, Kristl J (**2013**) The design trend in tissue-engineering scaffolds based on nanomechanical properties of individual electrospun nanofibers. *Int J Pharmaceut* 455: 338-347.
[35] Sonseca A, Peponi L, Sahuquillo O, Kenny JM, Gimenez E (**2012**) Electrospinning of biodegradable polylactide/hydroxyapatite nanofibers: Study on the morphology, crystallinity structure and thermal stability. *Polym Degrad Stabil* 97: 2052-2059.